BIOCHEMISTRY
including biophysical chemistry & molecular biology

Article

pubs.acs.org/biochemistry

Identification of the Dimer Interface of a Bacterial Ca^{2+}/H^+ Antiporter

Marc Ridilla,[†] Anoop Narayanan,[†] Jeffrey T. Bolin, and Dinesh A. Yernool*

Department of Biological Sciences, Purdue University, 240 South Martin Jischke Drive, West Lafayette, Indiana 47906, United States

Supporting Information

ABSTRACT: Members of the calcium/cation antiporter superfamily, including the cardiac sodium/calcium exchangers, are secondary active transporters that play an essential role in cellular Ca^{2+} homeostasis. A notable feature of this group of transporters is the high levels of sequence similarity in relatively short sequences constituting the functionally important α-1 and α-2 regions in contrast to relatively lower degrees of similarity in the extended adjoining sequences. This suggests a similar structure and function of core transport machinery but possible differences in topology and/or oligomerization, a topic that has not been adequately addressed. Here we present the first example of purification of a bacterial member of this superfamily (CAX^{CK31}) and analyze its quaternary structure. Purification of CAX^{CK31} required the presence of a choline headgroup-containing detergent or lipid to yield stable preparations of the monomeric transporter. H^+-driven Ca^{2+} transport was demonstrated by reconstituting purified CAX^{CK31} into liposomes. Dimeric CAX^{CK31} could be isolated by manipulation of detergent micelles. Dimer formation was shown to be dependent on micelle composition as well as protein concentration. Furthermore, we establish that CAX^{CK31} forms dimers in the membrane by analysis of cross-linked proteins. Using a dimeric homology model derived from the monomeric structure of the archaeal NCX homologue (Protein Data Bank entry 3V5U), we introduced cysteine residues and through cross-linking experiments established the role of transmembrane helices 2 and 6 in the putative dimer interface.

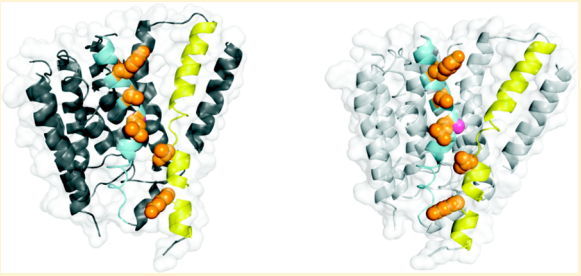

The calcium/cation antiporter (CaCA) superfamily comprises five families:[1] the NCX and NCKX families of animal Na^+/Ca^{2+} exchangers; the YRBG family of bacterial and archaeal exchangers, which takes its name from the *yrbG* gene in *Escherichia coli*; the CAX family of Ca^{2+}/H^+ exchangers found in yeasts, plants, archaea, and eubacteria; and the cation/Ca^{2+} exchangers, or CCX. Transporters belonging to the CaCA superfamily catalyze the following generalized transport equilibrium: $Ca^{2+}_{(in)} + [nH^+ \text{ or } nNa^+]_{(out)} \rightleftharpoons Ca^{2+}_{(out)} + [nH^+ \text{ or } nNa^+]_{(in)}$.[2] Other divalent cations are transported by various members of the superfamily.[3] The NCX family of transporters has been more extensively studied than any other family. Its members play a vital role in Ca^{2+} transport in excitable cells, namely, cardiac myocytes and neurons, where NCX malfunction has been implicated in various pathologies.[4−7]

On the basis of sequence analysis, it was predicted that CaCA superfamily members have a core transmembrane domain that includes at least nine transmembrane helices (Table 1), and many members probably have additional transmembrane helices decorating the central core.[1] The placement of the N- and C-termini with respect to the membrane is proposed to vary among families. Common to all members are two loops, designated α-1 and α-2, each containing a conserved G(S/T)SxP(D/E) motif. The level of conservation is generally greater in α-1 than in α-2.[8] The level of sequence conservation outside of these signature motifs is rather low within families and essentially nonexistent between families (Table 1). Given these large variations in sequence and topology between various families in the CaCA superfamily, an interesting question is whether quaternary structure is conserved within the superfamily.

Table 1. Sequence Similarity among Various Eukaryotic, Prokaryotic, and Archaeal CaCAs[a]

	% identity (% similarity) to NCX_Mj	% identity (% similarity) to NCX_Mj in α-1	% identity (% similarity) to NCX_Mj in α-2	predicted no. of TMs
Methanocaldococcus jannaschii (NCX_Mj)	100	100	100	9[b]
Caulobacter sp. K31 (CAX^{CK31})	5 (17)	16 (35)	15 (33)	11
Canis familiaris	2 (17)	35 (48)	28 (41)	10
E. coli	9 (25)	45 (58)	37 (52)	10
Vibrio cholerae	8 (22)	42 (52)	50 (57)	10
Homo sapiens	2 (15)	35 (48)	28 (41)	9
Drosophila melanogaster	3 (24)	35 (52)	37 (46)	11

[a]Amino acid sequences representing either full-length protein or the α-1 or α-2 repeat from each were compared to that of NCX_Mj using ClustalW2. Numbers of transmembrane helices (TMs) were predicted using PHDhtm. [b]The crystal structure of NCX_Mj (PDB entry 3V5U) has 10 TMs.

A YRBG family transporter from *M. jannaschii* (NCX_Mj) was recently crystallized as a monomer;[9] however, the apparent

Received: September 5, 2012
Revised: November 6, 2012
Published: November 7, 2012

   dx.doi.org/10.1021/bi3012109 | *Biochemistry* 2012, 51, 9603−9611

sufficiency of the crystallographic monomer to potentially meet the requirements for transport does not preclude an oligomeric native state.[10] For example, the crystal structures of NhaA,[11,12] the H^+/Cl^- exchange transporter,[13] and TrkH[14] reveal ion pathways in each monomer, but the transporters exist as physiological dimers that, in many cases, provide additional functions.[15−17] Conflicting results have kept the true oligomerization state of glucose transporter GLUT1 in question for many years.[18−20] Moreover, the ADP/ATP carrier has been crystallized in both monomeric[21] and native dimeric[22] states from protein purified by identical methods.

This study presents the first overexpression and purification of a member of the CAX family, demonstrates H^+-driven Ca^{2+} transport, demonstrates the presence of dimers in membranes, identifies a detergent mixture that yields concentration-dependent dimerization in solution after purification, and identifies the dimer interface through model-directed mutagenesis and chemical cross-linking.

EXPERIMENTAL PROCEDURES

Cloning and Expression. A CAX family gene from *Caulobacter* sp. K31 (accession number ZP-01418997), herein termed CAX^{CK31}, was selected from our previous large-scale screen to identify prokaryotic CaCA that can be overexpressed in *E. coli*.[23] DNA encoding residues 1−416 was amplified via polymerase chain reaction (PCR) and cloned into vector pETCTGFP.[23] The resulting clone was capable of producing a CAX^{CK31}-GFP-His_{11} fusion protein containing C-terminal green fluorescent protein and an undecahistidine tag. For Förster resonance energy transfer (FRET) experiments, GFP was replaced with monomeric cherry-red fluorescent protein (mCherry), which forms a FRET pair with GFP-fused CAX^{CK31} protein. Cysteine residues were introduced by site-directed mutagenesis using the overlap PCR method; wild-type CAX^{CK31} contains no cysteine residues.

The restrained-expression method was used to produce fusion proteins.[23] Briefly, cultures grown at 37 °C to an optical density of 0.6 at 600 nm were cooled to 25 °C, and target gene expression was initiated by addition of 0.01% (w/v) arabinose. Expression continued for 20 h at 25 °C. Cells were harvested by centrifugation for 15 min at 5250*g*.

Isolation of *E. coli* Membranes. Cell pellets were resuspended in buffer A [20 mM Tris-HCl (pH 8.0) and 300 mM NaCl] and lysed using an Emulsiflex-C3 (Avestin Inc.) with a homogenizing valve pressure of 15000−20000 lb/in.^{2}. Large debris was removed from the lysate by centrifugation for 30 min at 5000*g*, and the resulting supernatant was centrifuged for 60 min at 180000*g* to sediment the membrane fraction.

Detergent Screening. The fluorescence size exclusion chromatography (FSEC) method[24] was used to identify detergents capable of extracting protein from membrane and maintaining it in stable form. Briefly, 0.5 mL of a 0.1 g/mL suspension of membrane in buffer A was solubilized using 100 × CMC detergents with a variety of headgroups and acyl chain lengths. After being extracted at 4 °C for 2 h, the samples were clarified by centrifugation, and supernatants were analyzed by FSEC using a Superdex-200 (S-200, GE Healthcare) column pre-equilibrated in the same detergent solution at 1 × CMC detergent. Detergents producing qualitatively Gaussian peaks were considered for purification and further analysis. In addition to individual detergents, detergent mixtures were also used to determine the optimal conditions for solubilization and purification of the protein. All results were reproduced at least three times; chromatograms shown are representative examples.

Purification. The isolated membrane was resuspended in buffer A at 0.1 g/mL, and protein was extracted with 100 × CMC *n*-dodecyl β-D-maltopyranoside (DDM) at 4 °C for 2 h. Extracts were clarified by centrifugation at 180000*g*, and His-tagged protein was incubated with 10% (v/v) TALON Co^{2+} affinity resin (BD Bioscience Inc.). The resin was packed into a column and washed with 4 column volumes of buffer B [buffer A with 1.5 mM Fos-Choline-12 (FC12)] or buffer C [buffer A with 0.75 mM FC12 and 0.01% (w/v) polyoxyethylene(8)-dodecyl ether ($C_{12}E_8$)] containing 10 mM imidazole, and then 4 column volumes of buffer B or C containing 25 mM imidazole. Protein was eluted from the resin with buffer B or C containing 300 mM imidazole. CAX^{CK31} was cleaved from GFP-His_{11} by incubation with 10% (w/w) TEV protease for 16 h at 4 °C, and cleavage products were separated by size-exclusion chromatography on a 10 mm × 300 mm S-200 column in buffer B or C.

Circular Dichroism Spectroscopy. Purified CAX^{CK31} (lacking tags) at 1.0 mg/mL (22.6 μM) was used in buffer B. Spectra were collected with a Chirascan CD spectrometer (Applied Photophysics) at 20 °C from 250 to 190 nm using a quartz cuvette with a 0.1 mm optical path, a 0.5 nm step size, a 2 nm bandwidth, and a 2 s averaging time. Each spectrum was the average of five scans. The secondary structure was calculated with K2D3[25] and compared with that predicted from sequence by PROFsec.[26]

Reconstitution and Ca^{2+} Transport Assay. Proteoliposome preparation proceeded primarily by the protocols published by Gaillard et al.[27] Briefly, a 6:6:3:3:1 mixture of chloroform solutions of POPC, POPE, POPS, SM, and PI (1-palmitoyl-2-oleoyl-*sn*-glycero-3-phosphocholine, 1-palmitoyl-2-oleoyl-*sn*-glycero-3-phosphoethanolamine, 1-palmitoyl-2-oleoyl-*sn*-glycero-3-phospho-L-serine, sphingomyelin, and L-α-phosphatidylinositol, respectively) was dried by rotary evaporation for 16 h and then resuspended in a 10 mM HEPES/Tris mixture (pH 7.0) and 140 mM choline chloride. The suspension was repeatedly (10 times) flash-frozen in liquid nitrogen and thawed and then extruded through a 0.2 μm filter 10 times. Purified CAX^{CK31} was added at a 1% (w/w) ratio of protein to lipid, and lipid vesicles were destabilized with 3:16 (w/w) FC12 to allow protein incorporation. FC12 was removed by three 2 h treatments with 80 mg/mL Bio-Beads (Bio-Rad, Hercules, CA) followed by centrifugation and resuspension in the appropriate internal buffer [10 mM HEPES/Tris mixture (varying pH), 140 mM choline chloride (or NaCl), and 100 μM Fura-2]. Proteoliposomes were again flash-frozen and thawed to allow penetration of internal buffer, extruded through a 0.2 μm filter 10 times, and harvested by centrifugation. Transport of Ca^{2+} was analyzed by addition of 100 μM $CaCl_2$ to a liposome suspension at 25 °C in a UVT acrylic cuvette (Evergreen Scientific), and the changes in the emission of Fura-2 at 510 nm upon excitation at 340 and 380 nm were continuously monitored using a FluoroMax-3 spectrofluorometer (HORIBA Jobin Yvon). The ratio of emission intensities at the two excitation wavelengths was computed and converted to Ca^{2+} concentration using a standard curve. The range between a baseline defined before addition of $CaCl_2$ and a systemic equilibrium obtained at the end of each assay by disrupting the liposomes with 0.003% (v/v) Triton X-100 represents the range from 0 to 100 μM Ca^{2+}.

dx.doi.org/10.1021/bi3012109 | *Biochemistry* 2012, 51, 9603−9611

Liposomes prepared without CAX^{CK31} served as a negative control.

Glutaraldehyde Cross-Linking. Glutaraldehyde cross-linking was conducted in buffer C with HEPES substituted for Tris, as glutaraldehyde reacts with Tris. Purified CAX^{CK31} at 1.0 mg/mL (22.6 μM) was incubated with 1.0−2.5 mM glutaraldehyde for 5 min at room temperature, and the reaction was terminated by the addition of 100 mM Tris-HCl (pH 8.0).

Copper Phenanthroline Cross-Linking. Purified CAX^{CK31}-F92C or CAX^{CK31}-F92C/R246C at 1.0 mg/mL (22.6 μM) or 0.1 g/mL suspensions of membranes [in 20 mM Tris (pH 8.0) and 300 mM NaCl] isolated from *E. coli* were incubated with 3 mM copper phenanthroline for 30 min at room temperature to catalyze disulfide bond formation between cysteines. After cross-linking in membranes, CAX^{CK31}-GFP was extracted with 1.5% (w/v) FC12 before sodium dodecyl sulfate−polyacrylamide gel electrophoresis (SDS−PAGE).

Analysis of Cross-Linked Samples. Cross-linked samples were analyzed by SDS−PAGE and MALDI-TOF mass spectrometry. Unpurified membrane samples analyzed by SDS−PAGE were visualized by Western blotting using a pentahistidine primary antibody and an AlexaFluor683-conjugated secondary antibody. Purified samples were visualized by Coommassie Blue staining. All blots were repeated several times to ensure reproducibility, and representative examples are shown.

FRET. For FRET experiments, purified fusion proteins CAX^{CK31}-GFP and CAX^{CK31}-mCherry were mixed at various ratios and concentrations in buffer C. To correct for the background of CAX^{CK31}-GFP homodimers and CAX^{CK31}-mCherry homodimers, the methods described by Scheu et al.[28] were employed. Briefly, mixtures of CAX^{CK31}-GFP and CAX^{CK31}-mCherry were prepared in various ratios, and fluorescence spectra corresponding to donor fluorescence (GFP; ex_{395}/em_{509}), acceptor fluorescence (mCherry; ex_{585}/em_{610}), and FRET (ex_{395}/em_{610}) were recorded for each mixture. Calculated FRET efficiencies[28] should be inversely and linearly proportional to the donor fraction if true FRET occurs. Measurements were taken using 0.1 mg/mL (2.3 μM), 5.0 mg/mL (113.1 μM), and 10.0 mg/mL (226.2 μM) CAX^{CK31} (total concentrations) to evaluate the concentration dependence of CAX^{CK31} dimerization.

SEC−MALS. Multiangle laser light scattering (MALS) data were collected during elution of purified CAX^{CK31} from an S-200 SEC column in buffer C. The UV (280 nm) absorbance, static multiangle laser light scattering, and differential refractive index were monitored by an in-line spectrophotometer (Agilent Technologies), miniDAWN TREOS (Wyatt Technology Corp.), and Optilab T-rEX (Wyatt Technology Corp.), respectively, and data were collected using ASTRA. Weight-average molecular masses for the polypeptide and detergent components of protein−detergent complexes were calculated by the previously described "three-detector method"[29−32] from data collected at the CAX^{CK31} elution peak. SEC−MALS was analyzed at multiple CAX^{CK31} concentrations ranging from 0.1 mg/mL (2.3 μM) to 10.0 mg/mL (226.2 μM) to demonstrate the concentration dependence of dimerization. Data presented are from single runs with CAX^{CK31}; error estimates arise from internal controls used in the three-detector method calculations.[29−32]

Hypothetical Model of Dimeric CAX^{CK31}. A TM-COFFEE[33] sequence alignment of CAX^{CK31} and NCX_Mj was supplied to MODELLER[34] along with the structure of NCX_Mj (PDB entry 3V5U[9]) to create a molecular model of the CAX^{CK31} monomer. The model was checked to ensure that it obeys the *cis*-positive rule.[35] Two monomers were then manipulated assuming 2-fold molecular symmetry about an axis perpendicular to the plane of the membrane until a visually reasonable fit was achieved. The dimer model was then subjected to 1000 rounds of structure idealization using REFMAC5[36] in the CCP4 software suite.[37]

RESULTS

Surfactants and Lipids Containing the Choline Headgroup Stabilize Purified CAX^{CK31}-GFP-His_{11}. Identification and optimization of expression of CAX^{CK31} were described previously.[23] Multiple detergents and mixtures were screened to identify candidates that would (i) effectively solubilize the protein of interest from membranes and (ii) stabilize the protein in solution in the absence of bulk lipids. Screening identified DDM as the most effective detergent for extracting the CAX^{CK31}-GFP-His_{11} fusion protein from membranes (data not shown). Although a Gaussian SEC profile was observed immediately after extraction with DDM, storage after extraction and purification resulted in aggregation of the fusion protein (Figure 1A). To stabilize the protein, various types of lipids (at 0.01 mg/mL) were added to DDM-containing buffers. The fusion protein was more stable in the presence of phosphatidylcholine (PC) than in other lipid/DDM mixtures (Figure 1B). To explore this observation, we used DDM-containing buffer supplemented with choline chloride salt. The SEC profile changed from an aggregated protein eluting at the void volume in DDM to a peak centered at 27 min when augmented with choline chloride, suggesting that the choline moiety plays some role in stabilizing the protein (Figure 1C). However, the SEC peak width at half-maximum was broader than in a DDM/PC mixture, suggesting the acyl chain may also play a role. Therefore, SEC analysis was conducted in buffers containing lipidlike detergents Fos-Choline-12 and LysoFos Choline 12 (LysoFC12). Both detergents exhibited symmetric

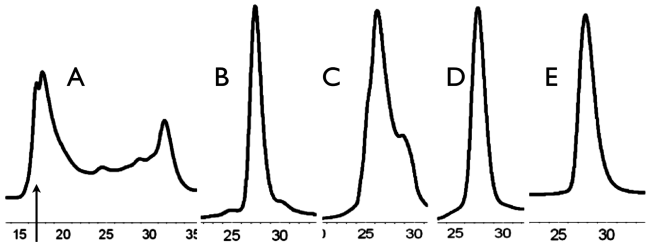

Figure 1. Effect of surfactants on the stability of CAX^{CK31} in solution. CAX^{CK31} was purified and analyzed by SEC in a selection of detergents or detergent/lipid mixtures: (A) DDM, (B) DDM and phosphatidylcholine, (C) DDM and choline chloride, (D) Fos-Choline-12, and (E) LysoFos Choline 12. The *X*- and *Y*-axes represent elution time in minutes and protein elution monitored by A_{280}, respectively. Peak heights have been normalized for the sake of clarity. CAX^{CK31} aggregates in DDM (A) as indicated by elution at the void volume of the column indicated by an arrow at 17 min. In contrast, the protein elutes in choline-containing detergents as a single, Gaussian peak revealing a stable preparation (D and E). Supplementing DDM with either the choline-containing lipid phosphatidylcholine (B) or the salt choline chloride (C) produces a qualitatively superior (i.e., lack of aggregation, fewer peaks, and decreased peak width at half-height) SEC profile compared to that of DDM alone.

dx.doi.org/10.1021/bi3012109 | *Biochemistry* 2012, 51, 9603−9611

peaks in SEC analysis, suggesting the fusion protein was stable in these detergents (Figure 1D,E). Nevertheless, the ability of choline-containing detergents to extract the protein from membranes was poor. A combination of extraction with DDM (100 × CMC) and subsequent replacement with FC12 (1.5 × CMC) proved to the best for the extraction, purification, and stabilization of the fusion protein. Purified CAX^{CK31} lacking tags migrates as a single band at the expected monomer mass of 44.2 kDa via SDS−PAGE (Figure 2A, inset) and produces a

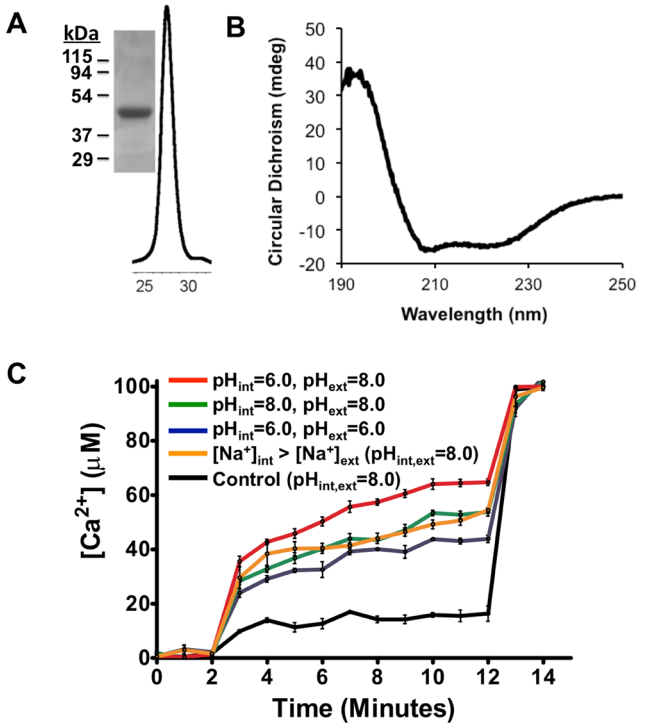

Figure 2. Characterization of purified CAX^{CK31}. (A) Purified CAX^{CK31} analyzed by SEC in FC12-containing buffer. The inset shows SDS−PAGE analysis. (B) Circular dichroism spectrum of purified CAX^{CK31}. (C) Proton-driven, pH-dependent Ca^{2+} transport by reconstituted CAX^{CK31}. The transport of Ca^{2+} into liposomes loaded with Fura-2 by CAX^{CK31} (colored lines) was monitored via changes in Fura-2 fluorescence after addition of Ca^{2+} to the bulk solution at 2 min. The pH values inside and outside the liposomes are denoted pH_{int} and pH_{ext}, respectively. The orange trace shows no stimulation of Ca^{2+} import by an outward-directed Na^+ gradient. The entry of Ca^{2+} into control liposomes lacking protein at pH 8.0 is shown in black. Data are means and the standard error of the mean of three replicate experiments.

single, Gaussian peak via SEC (Figure 2A), suggestive of a monodisperse preparation. Circular dichroism spectra (Figure 2B) revealed that purified CAX^{CK31} in FC12 contains secondary structure matching predictions from sequence analysis (74% α and 2.9% β).

Purified CAX^{CK31} Retains Transport Function. The functional integrity of purified CAX^{CK31} was established by reconstitution into liposomes and Ca^{2+} transport analysis. Proteoliposomes accumulated more Ca^{2+} than control liposomes lacking protein (Figure 2C). Ca^{2+}/H^+ exchange in the absence of Na^+ is demonstrated by the greater level of accumulation of Ca^{2+} in the lumen of liposomes with an outward-directed proton gradient than in liposomes having the same pH on both sides (i.e., lower pH inside increased Ca^{2+} influx). Furthermore, an outward-directed Na^+ gradient (under symmetrical pH conditions at pH 8.0) does not lead to an increased rate of Ca^{2+} transport over liposomes in the absence of Na^+ under the same pH conditions, demonstrating that Na^+ has no effect on Ca^{2+} transport. These data suggest that CAX^{CK31} is not a Na^+/Ca^{2+} exchanger but a H^+-driven Ca^{2+} transporter. In the absence of a proton gradient (i.e., the same pH on both sides of the membrane), alkaline pH stimulated Ca^{2+} transport, a behavior that is similar to the pH-dependent activation of cardiac NCX,[38] indicating similarities in transport characteristics between the two proteins in addition to similarities in primary sequence. The SEC profile and transport activities remained the same as those of the fresh protein after storage for at least 1 week at 4 °C, indicating the preparation is stable in FC12 detergent. SEC analysis of CAX^{CK31} at protein concentrations of >5.0 mg/mL (113.1 μM) showed a small peak with a larger hydrodynamic radius suggestive of oligomerization (data not shown).

CAX^{CK31} Is a Dimer in Membranes. To analyze the oligomeric state of CAX^{CK31} in lipid bilayers, we mutated residues F92 and R246 to introduce cysteines into the previously cysteine-free protein; these positions were chosen on the basis of a previous study of oligomerization of cardiac NCX.[39] *E. coli* membranes containing the CAX^{CK31}-F92C/R246C-GFP double mutant treated with copper phenanthroline were analyzed by Western blotting. The three distinct species observed match the pattern reported by Ren et al.[39] and were likewise interpreted as an intermolecularly cross-linked dimer, a non-crosslinked-monomer, and an intramolecularly cross-linked monomer (Figure 1 of the Supporting Information). Increased mobility of intramolecularly cross-linked species in nonreducing SDS−PAGE is generally attributed to either compaction of the molecule by the covalent bond between introduced cysteine side chains well-separated in primary sequence[40] or incomplete unfolding in SDS also due to the bond.[41] This pattern of disulfide cross-linking is maintained in a detergent solution for the purified CAX^{CK31}-F92C/R246C double mutant lacking the GFP tags (Figure 3). The CAX^{CK31}-

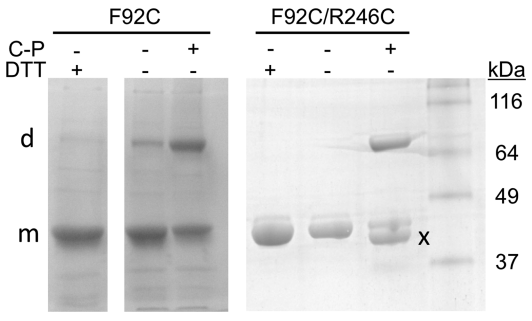

Figure 3. Cross-linking of CAX^{CK31} in solution via introduced cysteine residues. SDS−PAGE analysis of purified CAX^{CK31}-F92C and CAX^{CK31}-F92C/R246C treated with 3 mM copper phenanthroline. The abbreviations d, m, and x represent the intermolecularly cross-linked dimer, the non-cross-linked monomer, and the intramolecularly cross-linked monomer, respectively.

R246C single mutant could not be overexpressed at sufficient levels and therefore was not used in this analysis. Cross-linking of the F92C single mutant produced exclusively intermolecular cross-links (Figure 3). Disulfide-linked CAX^{CK31}-F92C was also analyzed by MALDI-TOF mass spectrometry, which revealed two major peaks at m/z values consistent with singly ionized dimeric and monomeric CAX^{CK31} (data not shown). These

dx.doi.org/10.1021/bi3012109 | *Biochemistry* 2012, 51, 9603−9611

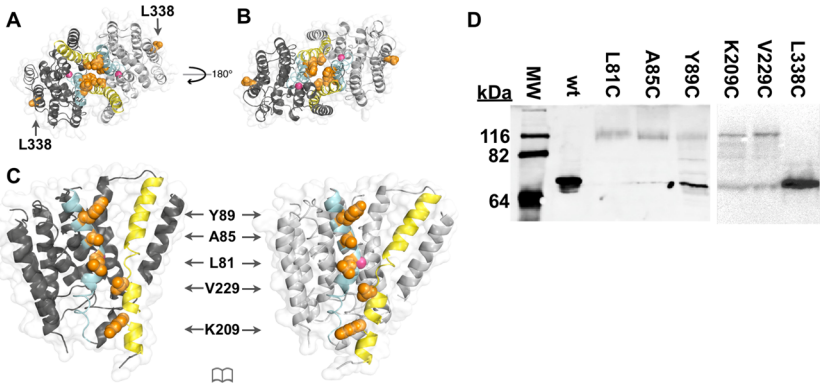

Figure 4. CAX^{CK31} dimer interface. (A) Hypothetical model of the CAX^{CK31} dimer viewed from the extracellular side. A homology model of CAX^{CK31} was generated using the structure of *M. jannaschii* NCX (PDB entry 3V5U), and two monomers were positioned with the proposed dimer interface made of TM2 (blue) and TM6 (yellow). Ca^{2+} atoms are colored magenta, and positions of Cys mutations are colored orange. The L338C mutation was not expected to form intermolecular cross-links because of its distance from the proposed interface. (B) View from the cytoplasm. (C) Open book representation of the dimer model. (D) Cross-linking of single-cysteine mutants of CAX^{CK31} in *E. coli* membranes. Isolated membranes from *E. coli* expressing CAX^{CK31}-GFP, CAX^{CK31}-L81C-GFP, CAX^{CK31}-A85C-GFP, CAX^{CK31}-Y89C-GFP, CAX^{CK31}-K209C-GFP, CAX^{CK31}-V229C-GFP, or CAX^{CK31}-L338C-GFP were treated with copper phenanthroline to promote disulfide bond formation. Western blotting of treated membranes reveals the characteristic intermolecular cross-links seen with purified CAX^{CK31}.

results show that CAX^{CK31} assembles into dimers in membranes, and the dimeric state can be stabilized in solution by cysteine cross-links.

The Conserved α-1 and α-2 Regions Are Close to the Dimer Interface. Residues F92 and R246 of CAX^{CK31} are within the conserved α-1 and α-2 repeats, respectively (Figure 2 of the Supporting Information). Equivalent residues map to the carboxyl-terminal ends of transmembrane helices 2 (TM2) and 6 (TM6) at the extracellular face of the monomeric structure of the archaeal NCX_Mj structure with the side chains pointing away from the protein core.[9] Inter- and intramolecular cross-linking in the F92C/R246C double mutant of CAX^{CK31} suggests that α-repeats are close both to each other within the monomer and to the dimer interface and is in agreement with the studies of cardiac NCX by Ren et al.[39] To further explore this putative dimer interface, we generated a hypothetical model of the NCX dimer (Figure 4A–C) and selected a series of residues near the symmetry axis and spanning the membrane for replacement with cysteines. Residues L81C, A85C, and Y89C map onto TM2C of the model, whereas K209C and V229C are on TM6. Each of five single mutants can be cross-linked with copper phenanthroline, whereas a cysteine introduced on the opposite side of the protein (L338C) does not form intermolecular cross-links (Figure 4D). The summation of disulfide cross-linking results strongly suggests that TM2 and TM6 form the dimer interface that extends from the extracellular side to the cytoplasmic surface.

Dimeric CAX^{CK31} Can Be Purified by Manipulating the Detergent Micelles. Dimeric CAX^{CK31} in membranes is converted into a monomer during purification in FC12. We screened various reagents that alter the FC12 detergent micelles to produce CAX^{CK31} with its native quaternary structure preserved. A mixture of 0.75 mM FC12 and 0.01% (w/v) $C_{12}E_8$ detergent was identified that yielded a mixture of monomer and dimer upon glutaraldehyde cross-linking at moderate protein concentrations (1.0 mg/mL, 22.6 μM) (Figure 5A). This suggested that the protein may be in monomer–dimer equilibrium. However, glutaraldehyde treatment at higher protein concentrations was deemed inadvisible because of the possibility of nonspecific cross-linking. Therefore, further assessment of dimerization was conducted by SEC

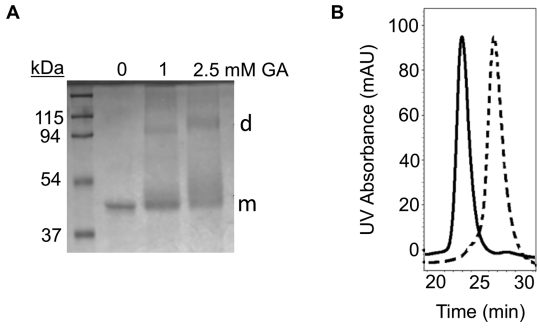

Figure 5. Dimerization of CAX^{CK31} purified in an FC12/$C_{12}E_8$ mixture. (A) SDS–PAGE analysis of CAX^{CK31} cross-linked (at 1 mg/mL) with 1.0 or 2.5 mM glutaraldehyde. Monomeric and dimeric species are denoted with m and d, respectively. (B) SEC elution chromatographs of 10 mg/mL CAX^{CK31} purified in FC12 (---) and FC12 and $C_{12}E_8$ (—). Earlier elution of the $C_{12}E_8$-containing protein–detergent complex was attributed to dimerization.

at 10.0 mg/mL (226.2 μM), which yielded a single peak with a species with a larger hydrodynamic radius (Figure 5B). The larger species could be due to protein oligomerization or formation of mixed micelles of unknown mass. To resolve this ambiguity, we conducted FRET analysis.

For FRET experiments, we employed purified CAX^{CK31}-GFP and CAX^{CK31}-mCherry as the donor and acceptor, respectively (Förster radius of 51 Å), and used the methods outlined by Scheu et al.[28] to detect protein homodimers: homooligomerization is validated when the FRET efficiency increases linearly with an increase in the acceptor:donor ratio. As we had previously failed to detect any effect of the presence of a GFP tag on the behavior of NCX in SEC or calcium transport assays, we did not expect the presence of the tag to affect oligomerization in a detergent solution. At the lowest concentration tested (0.1 mg/mL, 2.3 μM), the FRET efficiency increased with an increase in acceptor fraction (Figure 6A), indicating formation of oligomers. The FRET efficiencies were significantly greater at higher protein concentrations [5.0 mg/mL (113.1 μM) and 10.0 mg/mL (226.2 μM)], indicating that oligomerization in detergent solutions is concentration-dependent.

dx.doi.org/10.1021/bi3012109 | *Biochemistry* 2012, 51, 9603–9611

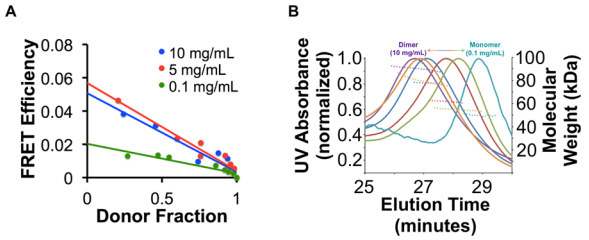

Figure 6. Dependence of oligomer formation on protein concentration. (A) FRET analysis of CAX^{CK31} oligomer formation in solution. FRET efficiencies for mixtures of CAX^{CK31}-GFP and CAX^{CK31}-mCherry were determined at various donor:acceptor ratios and different total CAX^{CK31} concentrations. FRET due to dimerization is confirmed by the linear relationship between FRET efficiency and donor fraction. The concentration dependence of CAX^{CK31} dimerization is demonstrated by increased efficiencies at greater CAX^{CK31} concentrations. (B) Analysis of the concentration dependence of CAX^{CK31} oligomerization by SEC–MALS. CAX^{CK31} was analyzed at 10.0 (purple), 8.0 (orange), 5.0 (blue), 2.0 (red), 1.0 (green), and 0.1 mg/mL (teal). The change in elution time demonstrates a change in the weight-average molecular mass of the concentration-dependent CAX^{CK31} monomer–dimer equilibrium mixture. Solid lines represent normalized UV absorbance (280 nm) of eluting CAX^{CK31}; dashed lines represent weight-average molecular masses (right axis) calculated at each time point during CAX^{CK31} elution using a combination of UV absorbance, laser light scattering, and differential refractive index measurements.

To characterize the dimerization of CAX^{CK31} in the absence of GFP or mCherry tags, we employed SEC–MALS. The three-detector method[29−32] allows estimation of the molecular mass of the polypeptide and detergent components of protein–detergent complexes (PDCs) from SEC–MALS data. We applied this method to analyze CAX^{CK31} at multiple concentrations (Figure 6B). As the CAX^{CK31} concentration was increased from 0.1 mg/mL (2.3 μM) to 10 mg/mL (226.2 μM), the weight-average molecular mass of the eluting species increased from 44.2 kDa (monomer) to 88.4 kDa (dimer) (Table 2). This is also evident from the shift in the time of elution from 29 to 26.5 min. Although neither FRET nor SEC–MALS can identify the exact fraction of CAX^{CK31} present in monomeric and dimeric forms, the weight-average molecular masses determined by SEC–MALS at the lowest and highest measurable CAX^{CK31} concentrations were approximately those expected for a CAX^{CK31} monomer and dimer, respectively, suggesting that the sample was almost completely monomeric or completely dimeric at those concentrations. The detergent:protein mass ratio in the CAX^{CK31}–FC12–$C_{12}E_8$ PDC was roughly 1:1, an expected value for integral membrane proteins, and slightly decreased in the dimer (0.84:1).

Table 2. Molecular Masses Calculated from SEC–MALS Data for CAX^{CK31} and the CAX^{CK31}–FC12–$C_{12}E_8$ Protein–Detergent Complex (PDC)

$[CAX^{CK31}]$ (mg/mL)	CAX^{CK31} molecular mass (kDa)	PDC molecular mass (kDa)	detergent:protein mass ratio
0.1	49.8 ± 4.0	102.3 ± 8.2	1.05
1.0	54.6 ± 4.4	107.9 ± 8.6	0.98
2.0	61.6 ± 4.9	120.0 ± 9.6	0.95
5.0	77.5 ± 6.2	144.9 ± 11.6	0.87
8.0	79.7 ± 6.4	154.4 ± 12.3	0.94
10.0	90.1 ± 7.2	166.0 ± 13.3	0.84

DISCUSSION

Many membrane proteins exist as homooligomeric and heterooligomeric complexes.[42] Defining their oligomerization state and maintaining that oligomeric state postpurification are nontrivial tasks, as illustrated by our studies of CAX^{CK31}. Extraction and postextraction stabilization of CAX^{CK31} required the use of DDM and FC12/LysoFC12, nonionic and zwitterionic surfactants, respectively. Although the use of a combination of detergents is not unusual, our additional studies are revealing. The extraction of CAX^{CK31} with DDM creates a unique constraint, a requirement for a choline-like moiety to maintain protein stability (Figure 1). Among the various lipids screened as supplements to DDM, only phosphatidylcholine was able to prevent protein aggregation. Although phosphatidylcholines are common lipids in eukaryotic cells, they are rarely present in bacteria and have not been reported in *E. coli*, our protein expression host.[43]

FC12 and the related lysolecithin-like detergent LysoFC12 are lipidlike detergents with single 12-carbon acyl chains connected to phosphocholine headgroups. They were developed to address the loss of stabilizing effects of lipids on membrane protein structure caused by solubilization in classical detergents.[44,45] Both of these detergents proved to be good replacements for mixed micelles of phosphatidylcholine and DDM during purification, resulting in significantly improved CAX^{CK31} stability, yielding monodisperse preparations. Furthermore, we demonstrate the importance of the surfactant headgroup in protein stability by using DDM supplemented with choline chloride salt. The requirement for the choline moiety holds only under conditions of detergent solubilization, as the protein was active in inverted vesicles made from *E. coli* membranes expressing CAX^{CK31}.[23] These data suggest that DDM extraction changes the protein, creating a putative binding site for a choline-like molecule. The generality of requirements for specific moieties after detergent extraction remains unknown. However, the Fos-Cholines were notably the most successful detergents in stabilizing a variety of membrane proteins in large-scale expression studies.[46−48]

Stabilization of CAX^{CK31} by FC12 comes at a price: it yields a monomer, a non-native state with respect to its quaternary structure in the membrane. A search for conditions that produce CAX^{CK31} dimers resulted in the identification of a mixture of FC12 and $C_{12}E_8$. The latter is a nonionic detergent with a large polyoxyethylene headgroup. The dependence on this specific detergent mixture and protein concentration to retain the dimeric state was demonstrated by FRET using CAX^{CK31}-GFP and CAX^{CK31}-mCherry. SEC–MALS confirmed that concentration-dependent dimer formation was mediated by the transporter by using protein lacking fusion tags and by a change in the detergent:protein mass ratio from 1.05 to 0.84 (Table 2) as the transporter concentration increased from 0.1 to 10 mg/mL, where they exist as monomer and dimer, respectively. The decrease in the detergent:protein ratio is expected when transporter molecules interact laterally via their transmembrane segments to displace detergent molecules. Broadly, the potential benefit of manipulation of detergent micelles to preserve the native oligomerization state of proteins is demonstrated by our studies.

CAX^{CK31} is the first bacterial member of the CaCA superfamily to be purified as monomers and dimers in solution. Recently, two archaeal homologues of the YRBG family were purified.[9,49] One of these proteins had more than one

dx.doi.org/10.1021/bi3012109 | *Biochemistry* 2012, 51, 9603–9611

aggregation state in solution; however, the aggregation states were not experimentally determined.[9] Previously, it was established that mammalian NCX and NCKX are dimers in membranes.[39,50,51] Both mammalian and archaeal NCX use Na^+ gradients to drive Ca^{2+} transport, whereas we show CAX^{CK31} to be a H^+/Ca^{2+} transporter. As for CAX^{CK31}, weakened function at acidic pH is also seen for cardiac NCX,[52] although the mechanism of proton sensing must be different as CAX^{CK31} does not possess the eukaryotic counterpart's cytoplasmic Ca^{2+}-binding domains. The altered specificity for the monovalent cation is consistent with the idea that the H^+ gradient is the major energy source for coupled transport in bacteria.[53] Despite the differences in substrate specificity, the central function of divalent/monovalent antiport activity is conserved in the CaCA superfamily.

The dimeric quaternary structure of CAX^{CK31} in membranes was established by cross-linking cysteines introduced at positions F92 and R246 of CAX^{CK31}, recapitulating studies of corresponding residues of cardiac NCX.[39] Despite the low overall level of sequence identity, this implied that (i) the relative positions of residues in the α-1 and α-2 regions of dog NCX and CAX^{CK31} are similar and (ii) these residues are close to the dimer interface. This analysis was extended by exploiting the recently determined archaeal NCX structure.[9] By modeling, we identified five additional residues on TM2 and TM6 near the symmetry axis of a putative dimer. The intermolecular disulfide cross-linking of introduced cysteines establishes the proximity of TM2 and TM6 to the intermolecular interface and suggests direct participation in dimer formation.

The determination of the crystal structure of the archaeal NCX was both a major feat and an advance in understanding the mechanism of transport.[9] Our identification of TM2 and TM6 as the dimer interface has impact on our understanding of the structure and function of these transporters. Three CAX^{CK31} residues that cross-link when mutated to cysteines, L81, A85, and Y89, map to TM2C of NCX_Mj where the equivalent residues are L52, L56, and Y60, respectively (Figure 7 and Figure 1A of the Supporting Information). These NCX_Mj residues, components of the conserved α-1 repeat, are neighbors of E54 that plays a central role in ion binding and transport. E54, which is situated on the opposite side of L52 and L56 within the same helical turn, coordinates the transported Ca^{2+} ion with two oxygens.[9] This places the Ca^{2+} binding site close to the protein−lipid acyl chain interface, a remarkable condition considering the more centrally located, protein-enclosed ion binding sites of other secondary transporters. Furthermore, the path from the extracellular side to the Ca^{2+} binding site was proposed to be delimited by TM2C, TM6, TM7, and bulk lipids, which would expose the acyl chains to water and ions, an unfavorable condition (Figure 7). These concerns can be resolved by considering our data of dimer formation with TM2 and TM6 at the interface. Such a dimer would have Ca^{2+} ions in each protomer and the ion permeation pathway leading to these ion binding sites surrounded by a protein core instead of bulk lipids. This implies that a common ion permeation pathway starts at the dimer interface on the extracellular side and bifurcates to reach the Ca^{2+} binding sites. Confirmation of this model awaits determination of a crystal structure of CAX^{CK31} in dimeric form.

Purification of monomeric and dimeric versions of the bacterial Ca^{2+}/H^+ antiporter emphasizes the role of detergent micelle manipulation in isolating membrane proteins in their native quaternary structures. The growing body of evidence of

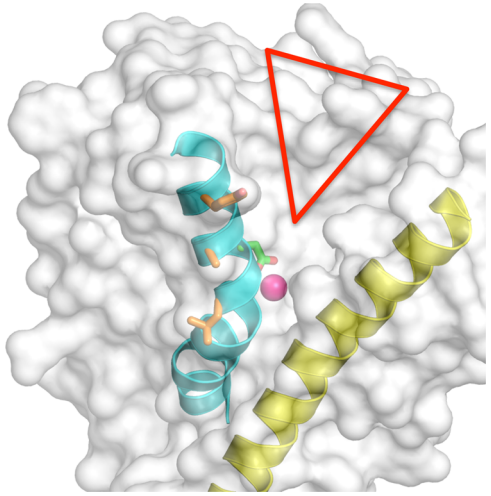

Figure 7. Relationship among the putative dimer interface, Ca^{2+} binding site, and Ca^{2+} permeation pathway. The structure of NCX_Mj (PDB entry 3V5U) is shown in surface representation with TM2 and TM6 colored cyan and yellow, respectively. Ca^{2+} is colored magenta and the Ca^{2+} coordinating residue E54 green. The interfacial residues L81, A85, and Y89 of CAX^{CK31} we identified are mapped onto equivalent positions in the NCX_Mj structure and are colored orange. The proposed Ca^{2+} entry passageway is denoted with a red triangle.

CaCA dimerization suggests that quaternary structure is indeed conserved in the superfamily despite the low overall level of sequence similarity. Our analysis also shows that Ca^{2+}/H^+ antiporters use the conserved α-repeats to support transport and oligomerization.

■ ASSOCIATED CONTENT

Supporting Information

Disulfide cross-linking of CAX^{CK31}-F92C/R246C-GFP in membranes (Figure 1) and sequence similarity among superfamily members in the α-1 and α-2 regions as well as a generalized topology schematic for the superfamily (Figure 2). This material is available free of charge via the Internet at http://pubs.acs.org.

■ AUTHOR INFORMATION

Corresponding Author

*Department of Biological Sciences, 240 S. Martin Jischke Dr., 333 Hockmeyer Hall, West Lafayette, IN 47907-2054. E-mail: dyernool@purdue.edu. Telephone: (765) 494-1960. Fax: (765) 496-1189.

Author Contributions

†M.R. and A.N. made equal contributions to this work.

Funding

This work was supported by National Institutes of Health Grant R01 GM093142 awarded to D.A.Y. M.R. was supported by National Institutes of Health Biophysics Training Grant 5T32GM008296.

Notes

The authors declare no competing financial interest.

■ ACKNOWLEDGMENTS

We acknowledge Lake N. Paul for his advice on SEC−MALS experiments and the use of the facilities of the Bindley Bioscience Center, a core facility of the National Institutes of

Health-supported Indiana Clinical & Translational Science Institute.

■ ABBREVIATIONS

$C_{12}E_8$, polyoxyethylene(8)dodecyl ether; CaCA, calcium/cation antiporter; DDM, *n*-dodecyl β-D-maltopyranoside; FC12, Fos-Choline-12; FRET, Förster resonance energy transfer; FSEC, fluorescence size exclusion chromatography; LysoFC12, LysoFos Choline 12; MALS, multiangle laser light scattering; PC, phosphatidylcholine; PDB, Protein Data Bank; PDC, protein−detergent complex; S-200, Superdex-200; TM, transmembrane helix.

■ REFERENCES

(1) Cai, X., and Lytton, J. (2004) The Cation/Ca^{2+} Exchanger Superfamily: Phylogenetic Analysis and Structural Implications. *Mol. Biol. Evol. 21*, 1692−1703.

(2) Saier, M. H., Jr., Tran, C. V., and Barabote, R. D. (2006) TCDB: The Transporter Classification Database for membrane transport protein analyses and information. *Nucleic Acids Res. 34*, D181−D186.

(3) Saier, M. H., Jr., Eng, B. H., Fard, S., Garg, J., Haggerty, D. A., Hutchinson, W. J., Jack, D. L., Lai, E. C., Liu, H. J., Nusinew, D. P., Omar, A. M., Pao, S. S., Paulsen, I. T., Quan, J. A., Sliwinski, M., Tseng, T.-T., Wachi, S., and Young, G. B. (1999) Phylogenetic characterization of novel transport protein families revealed by genome analyses. *Biochim. Biophys. Acta 1422*, 1−56.

(4) Blaustein, M. P., and Lederer, W. J. (1999) Sodium/Calcium Exchange: Its Physiological Implications. *Physiol. Rev. 79*, 763−854.

(5) Craner, M. J., Hains, B. C., Lo, A. C., Black, J. A., and Waxman, S. G. (2004) Co-localization of sodium channel Nav1.6 and the sodium−calcium exchanger at sites of axonal injury in the spinal cord in EAE. *Brain 127*, 294−303.

(6) Jeon, D., Yang, Y.-M., Jeong, M.-J., Philipson, K. D., Rhim, H., and Shin, H.-S. (2003) Enhanced Learning and Memory in Mice Lacking Na^+/Ca^{2+} Exchanger 2. *Neuron 38*, 965−976.

(7) Pott, C., Goldhaber, J. I., and Philipson, K. D. (2004) Genetic manipulation of cardiac Na^+/Ca^{2+} exchange expression. *Biochem. Biophys. Res. Commun. 322*, 1336−1340.

(8) Shigaki, T., Rees, I., Nakhleh, L., and Hirschi, K. D. (2006) Identification of three distinct phylogenetic groups of CAX cation/proton antiporters. *J. Mol. Evol. 63*, 815−825.

(9) Liao, J., Li, H., Zeng, W., Sauer, D. B., Belmares, R., and Jiang, Y. (2012) Structural Insight into the Ion-Exchange Mechanism of the Sodium/Calcium Exchanger. *Science 335*, 686−690.

(10) Veenhoff, L. M., Heuberger, E. H. M., and Poolman, B. (2002) Quaternary structure and function of transport proteins. *Trends Biochem. Sci. 27*, 242−249.

(11) Hunte, C., Screpanti, E., Venturi, M., Rimon, A., Padan, E., and Michel, H. (2005) Structure of a Na^+/H^+ antiporter and insights into mechanism of action and regulation by pH. *Nature 435*, 1197−1202.

(12) Herz, K., Rimon, A., Jeschke, G., and Padan, E. (2009) β-Sheet-dependent Dimerization Is Essential for the Stability of NhaA Na^+/H^+ Antiporter. *J. Biol. Chem. 284*, 6337−6347.

(13) Dutzler, R., Campbell, E. B., Cadene, M., Chait, B. T., and MacKinnon, R. (2002) X-ray structure of a ClC chloride channel at 3.0 Å reveals the molecular basis of anion selectivity. *Nature 415*, 287−294.

(14) Cao, Y., Jin, X., Huang, H., Derebe, M. G., Levin, E. J., Kabaleeswaran, V., Pan, Y., Punta, M., Love, J., Weng, J., Quick, M., Ye, S., Kloss, B., Bruni, R., Martinez-Hackert, E., Hendrickson, W. A., Rost, B., Javitch, J. A., Rajashankar, K. R., Jiang, Y., and Zhou, M. (2011) Crystal structure of a potassium ion transporter, TrkH. *Nature 471*, 336−340.

(15) Gärtner, R. M., Perez, C., Koshy, C., and Ziegler, C. (2011) Role of bundle helices in a regulatory crosstalk in the trimeric betaine transporter BetP. *J. Mol. Biol. 414*, 327−336.

(16) Rimon, A., Tzubery, T., and Padan, E. (2007) Monomers of the NhaA Na^+/H^+ antiporter of *Escherichia coli* are fully functional yet dimers are beneficial under extreme stress conditions at alkaline pH in the presence of Na^+ or Li. *J. Biol. Chem. 282*, 26810−26821.

(17) Robertson, J. L., Kolmakova-Partensky, L., and Miller, C. (2010) Design, function and structure of a monomeric ClC transporter. *Nature 468*, 844−847.

(18) Zottola, R. J., Cloherty, E. K., Coderre, P. E., Hansen, A., Hebert, D. N., and Carruthers, A. (1995) Glucose transporter function is controlled by transporter oligomeric structure. A single, intramolecular disulfide promotes GLUT1 tetramerization. *Biochemistry 34*, 9734−9747.

(19) Boulter, J. M., and Wang, D. N. (2001) Purification and characterization of human erythrocyte glucose transporter in decylmaltoside detergent solution. *Protein Expression Purif. 22*, 337−348.

(20) Carruthers, A., DeZutter, J., Ganguly, A., and Devaskar, S. U. (2009) Will the original glucose transporter isoform please stand up! *Am. J. Physiol. 297*, E836−E848.

(21) Pebay-Peyroula, E., Dahout-Gonzalez, C., Kahn, R., Trézéguet, V., Lauquin, G. J.-M., and Brandolin, G. (2003) Structure of mitochondrial ADP/ATP carrier in complex with carboxyatractyloside. *Nature 426*, 39−44.

(22) Nury, H., Dahout-Gonzalez, C., Trézéguet, V., Lauquin, G., Brandolin, G., and Pebay-Peyroula, E. (2005) Structural basis for lipid-mediated interactions between mitochondrial ADP/ATP carrier monomers. *FEBS Lett. 579*, 6031−6036.

(23) Narayanan, A., Ridilla, M., and Yernool, D. A. (2011) Restrained expression, a method to overproduce toxic membrane proteins by exploiting operator−repressor interactions. *Protein Sci. 20*, 51−61.

(24) Kawate, T., and Gouaux, E. (2006) Fluorescence-Detection Size-Exclusion Chromatography for Precrystallization Screening of Integral Membrane Proteins. *Structure 14*, 673−681.

(25) Perez-Iratxeta, C., and Andrade-Navarro, M. (2008) K2D2: Estimation of protein secondary structure from circular dichroism spectra. *BMC Struct. Biol. 8*, 25.

(26) Rost, B., Yachdav, G., and Liu, J. (2004) The PredictProtein server. *Nucleic Acids Res. 32*, W321−W326.

(27) Gaillard, I., Slotboom, D. J., Knol, J., Lolkema, J. S., and Konings, W. N. (1996) Purification and reconstitution of the glutamate carrier GltT of the thermophilic bacterium *Bacillus stearothermophilus*. *Biochemistry 35*, 6150−6156.

(28) Scheu, P. D., Liao, Y.-F., Bauer, J., Kneuper, H., Basche, T., Unden, G., and Erker, W. (2010) Oligomeric Sensor Kinase DcuS in the Membrane of *Escherichia coli* and in Proteoliposomes: Chemical Cross-linking and FRET Spectroscopy. *J. Bacteriol. 192*, 3474−3483.

(29) Hayashi, Y., Matsui, H., and Takagi, T. (1989) Membrane protein molecular weight determined by low-angle laser light-scattering photometry coupled with high-performance gel chromatography. In *Biomembranes Part S*, pp 514−528, Academic Press, San Diego.

(30) Folta-Stogniew, E., and Williams, K. R. (1999) Determination of molecular masses of proteins in solution: Implementation of an HPLC size exclusion chromatography and laser light scattering service in a core laboratory. *Journal of Biomolecular Techniques 10*, 51−63.

(31) Wen, J., Arakawa, T., and Philo, J. S. (1996) Size-Exclusion Chromatography with On-Line Light-Scattering, Absorbance, and Refractive Index Detectors for Studying Proteins and Their Interactions. *Anal. Biochem. 240*, 155−166.

(32) Yernool, D., Boudker, O., Folta-Stogniew, E., and Gouaux, E. (2003) Trimeric Subunit Stoichiometry of the Glutamate Transporters from *Bacillus caldotenax* and *Bacillus stearothermophilus*. *Biochemistry 42*, 12981−12988.

(33) Chang, J.-M., Di Tommaso, P., Taly, J.-F., and Notredame, C. (2012) Accurate multiple sequence alignment of transmembrane proteins with PSI-Coffee. *BMC Bioinf. 13* (Suppl. 4), S1.

(34) Sali, A., and Blundell, T. L. (1993) Comparative protein modelling by satisfaction of spatial restraints. *J. Mol. Biol. 234*, 779−815.

(35) von Heijne, G., and Gavel, Y. (1988) Topogenic signals in integral membrane proteins. *Eur. J. Biochem. 174*, 671−678.
(36) Vagin, A. A., Steiner, R. A., Lebedev, A. A., Potterton, L., McNicholas, S., Long, F., and Murshudov, G. N. (2004) REFMAC5 dictionary: Organization of prior chemical knowledge and guidelines for its use. *Acta Crystallogr. D60*, 2184−2195.
(37) Winn, M. D., Ballard, C. C., Cowtan, K. D., Dodson, E. J., Emsley, P., Evans, P. R., Keegan, R. M., Krissinel, E. B., Leslie, A. G. W., McCoy, A., McNicholas, S. J., Murshudov, G. N., Pannu, N. S., Potterton, E. A., Powell, H. R., Read, R. J., Vagin, A., and Wilson, K. S. (2011) Overview of the CCP4 suite and current developments. *Acta Crystallogr. D67*, 235−242.
(38) Doering, A. E., and Lederer, W. J. (1993) The mechanism by which cytoplasmic protons inhibit the sodium-calcium exchanger in guinea-pig heart cells. *J. Physiol. 466*, 481−499.
(39) Ren, X., Nicoll, D. A., Galang, G., and Philipson, K. D. (2008) Intermolecular Cross-Linking of Na^+−Ca^{2+} Exchanger Proteins: Evidence for Dimer Formation. *Biochemistry 47*, 6081−6087.
(40) Cumming, R. C., Andon, N. L., Haynes, P. A., Park, M., Fischer, W. H., and Schubert, D. (2004) Protein Disulfide Bond Formation in the Cytoplasm during Oxidative Stress. *J. Biol. Chem. 279*, 21749−21758.
(41) Santacruz-Toloza, L., Ottolia, M., Nicoll, D. A., and Philipson, K. D. (2000) Functional Analysis of a Disulfide Bond in the Cardiac Na^+-Ca^{2+} Exchanger. *J. Biol. Chem. 275*, 182−188.
(42) Dalbey, R. E., Wang, P., and Kuhn, A. (2011) Assembly of Bacterial Inner Membrane Proteins. *Annu. Rev. Biochem. 80*, 161−187.
(43) Sohlenkamp, C., López-Lara, I. M., and Geiger, O. (2003) Biosynthesis of phosphatidylcholine in bacteria. *Prog. Lipid Res. 42*, 115−162.
(44) Weltzien, H. U., Richter, G., and Ferber, E. (1979) Detergent properties of water-soluble choline phosphatides. Selective solubilization of acyl-CoA:lysolecithin acyltransferase from thymocyte plasma membranes. *J. Biol. Chem. 254*, 3652−3657.
(45) Garavito, R. M., Picot, D., and Loll, P. J. (1996) Strategies for crystallizing membrane proteins. *J. Bioenerg. Biomembr. 28*, 13−27.
(46) Carpenter, E. P., Beis, K., Cameron, A. D., and Iwata, S. (2008) Overcoming the challenges of membrane protein crystallography. *Curr. Opin. Struct. Biol. 18*, 581−586.
(47) Hammon, J., Palanivelu, D. V., Chen, J., Patel, C., and Minor, D. L., Jr. (2009) A green fluorescent protein screen for identification of well-expressed membrane proteins from a cohort of extremophilic organisms. *Protein Sci. 18*, 121−133.
(48) Lewinson, O., Lee, A. T., and Rees, D. C. (2008) The funnel approach to the precrystallization production of membrane proteins. *J. Mol. Biol. 377*, 62−73.
(49) Mercado Besserer, G., Nicoll, D. A., Abramson, J., and Philipson, K. D. (2012) Characterization and purification of a Na^+/Ca^{2+} exchanger from an Archaebacterium. *J. Biol. Chem. 287*, 8652−8659.
(50) John, S. A., Ribalet, B., Weiss, J. N., Philipson, K. D., and Ottolia, M. (2011) Ca^{2+}-dependent structural rearrangements within Na^+−Ca^{2+} exchanger dimers. *Proc. Natl. Acad. Sci. U.S.A. 108*, 1699−1704.
(51) Schwarzer, A., Kim, T. S. Y., Hagen, V., Molday, R. S., and Bauer, P. J. (1997) The Na/Ca-K Exchanger of Rod Photoreceptor Exists as Dimer in the Plasma Membrane. *Biochemistry 36*, 13667−13676.
(52) Boyman, L., Hagen, B. M., Giladi, M., Hiller, R., Lederer, W. J., and Khananshvili, D. (2011) Proton-sensing Ca^{2+} binding domains regulate the cardiac Na^+/Ca^{2+} exchanger. *J. Biol. Chem. 286*, 28811−28820.
(53) Harold, F. M., and Maloney, P. C. (1996) Energy Transduction by Ion Currents. In *Escherichia coli and Salmonella: Cellular and Molecular Biology*, pp 283−306, American Society for Microbiology Press, Washington, DC.